Smart Structures and Systems, *Vol. 13, No. 2 (2014) 219-233*
DOI: http://dx.doi.org/10.12989/sss.2014.13.2.219

Adaptive length SMA pendulum smart tuned mass damper performance in the presence of real time primary system stiffness change

Michael T. Contreras[1a], Dharma Theja Reddy Pasala[2b] and Satish Nagarajaiah[*3]

[1]*Jet Propulsion Laboratory, California Institute of Technology, Pasadena, CA 91109, USA*
[2]*Department of Civil and Environmental Engineering, Rice University, Houston, TX 77005, USA*
[3]*Department of Civil and Environmental Engineering and Mechanical Engineering and Material science, Rice University, Houston, TX 77005, USA*

(Received May 1, 2012, Revised May 9, 2013, Accepted May 10, 2013)

Abstract. In a companion paper, Pasala and Nagarajaiah analytically and experimentally validate the Adaptive Length Pendulum Smart Tuned Mass Damper (ALP-STMD) on a primary structure (2 story steel structure) whose frequencies are time invariant (Pasala and Nagarajaiah 2012). In this paper, the ALP-STMD effectiveness on a primary structure whose frequencies are time varying is studied experimentally. This study experimentally validates the ability of an ALP-STMD to adequately control a structural system in the presence of real time changes in primary stiffness that are detected by a real time observer based system identification. The experiments implement the newly developed Adaptive Length Pendulum Smart Tuned Mass Damper (ALP-STMD) which was first introduced and developed by Nagarajaiah (2009), Nagarajaiah and Pasala (2010) and Nagarajaiah *et al.* (2010). The ALP-STMD employs a mass pendulum of variable length which can be tuned in real time to the parameters of the system using sensor feedback. The tuning action is made possible by applying a current to a shape memory alloy wire changing the effective length that supports the damper mass assembly in real time. Once a stiffness change in the structural system is detected by an open loop observer, the ALP-STMD is re-tuned to the modified system parameters which successfully reduce the response of the primary system. Significant performance improvement is illustrated for the stiffness modified system, which undergoes the re-tuning adaptation, when compared to the stiffness modified system without adaptive re-tuning.

Keywords: smart tuned mass damper; adaptive passive tuned mass damper; tuned vibration absorbers; shape memory alloy; adaptive length pendulum; observer based structural health monitoring

1. Introduction

In recent years, significant attention has been dedicated to studying the effectiveness of Tuned Mass Dampers (TMDs) and Multiple Tuned Mass Dampers (MTMD). A TMD is a passive device

∗Corresponding author, Professor, E-mail: Satish.Nagarajaiah@rice.edu
[a] Technical Staff, Email: Michael.T.Contreras@jpl.nasa.gov
[b] Graduate Student, E-mail: drp1@rice.edu

http://www.techno-press.org/?journal=sss&subpage=8 ISSN: 1738-1584 (Print), 1738-1991 (Online)

that inherently dissipates energy from a structural system because its dynamic properties correspond to a dominant frequency in the structural system. As such, TMDs are very sensitive to their frequency tuning ratio even when designed properly. Also, a single TMD which has fixed dynamic properties is only capable of dissipating energy at a single dominant frequency of response. The MTMD is one way to overcome this limitation; however, the MTMD cannot be applied to time varying systems with damage or faults because they cannot be adaptively tuned in real time. In an effort to make TMDs and MTMDs more robust, TMDs with adjustable damping were first examined by Hrovat *et al.* (1983). The work of Hrovat led to the development of a several novel semiactive tuned mass dampers with variable damping by many other researchers.

Nagarajaiah and Varadarajan developed a Smart Tuned Mass Damper (STMD) with variable stiffness (Nagarajaiah and Varadarajan 2000) that was able to perform real time tuning through implementation of the Semi-Active Independent Variable Stiffness (SAIVS) device (Nagarajaiah, U.S. Patent No. 6,098,969). The patented system has been evaluated extensively both analytically and experimentally. The variation of stiffness of the STMD is made possible by an estimation of instantaneous frequency and a time frequency controller also developed by Nagarajaiah and Varadarajan (2000). Varadarajan and Nagarajaiah have also illustrated the power saving advantages of the STMD device by examining a tall benchmark building in which response reductions achieved were comparable to an active tuned mass damper while consuming orders of magnitude less power (Varadarajan and Nagarajaiah 2004).

Analytical studies on STMDs with variable damping have been performed by Abe and Igusa (1996). Experimentally, there have been several additional applications of semiactive technologies involving STMDs. Semiactive impact dampers were developed by Caughey and Karyeaclis and shown to be effective experimentally (Caughey and Karyeaclis 1989). Controllable Tuned Sloshing Dampers (CTSD) and Controllable Tuned Liquid Column Dampers (CTLCD) have also been proposed and are implemented in full scale applications. Lou *et al.* proposed a CTSD device which extends a passive Tuned Sloshing Damper (TSD) in which the length of a sloshing tank can be modified, thus increasing the adaptivity of the device (Lou *et al.* 1994). Also, Abe *et al.* and Yalla *et al.* have developed a semiactive CTLCD device based on a TLCD with an added variable orifice for increased robustness (Abe and Igusa 1996, Yalla *et al.* 2001). Additionally, there are SMTDs which implement the variable damping capability of Magneto-Rheological (MR) dampers for re-tuning, and they have been demonstrated by simulation (Weber *et al.* 2011). Along with the variety of STMD actuators that have been developed, algorithms have been proposed to controls them in real time. Recently, Occhiuzzi *et al.* have developed control algorithms to re-tune a STMD to enhance performance on a vibrating footbridge (Occhiuzzi *et al.* 2008) and Hazra *et al.* have developed control algorithms based on blind identification to re-tune a STMD on a laboratory structure (Hazra *et al.* 2010).

In practice, there have been several successful full scale implementations of Adaptive Passive Tuned Mass Dampers (APTMD). APTMDs possess the adaptability of an STMD; however, their adaptation is performed offline usually through adjustments in geometric configuration. They have been successfully implemented in the Citicorp Center building (New York City) through the use of nitrogen springs (Peterson 1980), and the Tokyo Tower through the use of an adaptive radius configuration (Koike and Tanida 1998).

The Adaptive Length Pendulum (ALP) is a pendulum mass system whose length can be adjusted to obtain the enhanced, online performance which is lacking in the APTMD. The APTMD methodology lays the foundation for development of the ALP-STMD which was first introduced

by Nagarajaiah (2009). The ALP concept has been utilized by Mekki *et al.* in which an alternator and gear configuration was introduced (Mekki *et al.* 2011), and by Roffel *et al.* in which a three dimensional application using adjustable air dampers was considered (Roffel *et al.* 2010, Roffel *et al.* 2011). This study employs the adaptive benefits of Shape Memory Alloy (SMA) wire in a new ALP-STMD configuration to experimentally compensate for primary system stiffness changes.

In summary, the benefits and limitations of different types of TMDs were discussed. Recalling that although APTMDs are capable of adaptive tuning to system parameters based on mechanical and/or physical changes to their configuration, they do not benefit from the real time sensor feedback and actuation found in STMDs. In a companion paper, Pasala and Nagarajaiah analytically and experimentally validate the ALP-STMD on a primary structure (2 story steel structure) whose frequencies are time invariant (Pasala and Nagarajaiah 2012). In this paper, the ALP-STMD effectiveness on a primary structure whose frequencies are time varying is studied experimentally. The main motivation of this experimental study is to demonstrate that by using a SMA in an ALP configuration, an ALP-STMD attains an enhanced level of robust adaptivity with respect to traditional APTMDs. The enhanced merits of the ALP-STMD are demonstrated by performing structural control in the presence of primary system stiffness change.

The stiffness change considered in this study is produced by a complete loss of tension in cable braces placed on both stories that provide strength in the lateral direction of loading. This severe event produces large primary structure frequency shifts of approximately 42%. Comparable and greater frequency changes have been observed in the identified vibration frequencies of real structures which are sensitive to soil structure interaction effects and earthquake ground motions (Meli *et al*. 1998, Muria-Vila *et al.* 2000). It is important to note that smaller decreases in frequency could be compensated for by using the proposed observer formulation and re-tuning the SMA pendulum using shorter lengths; however, the bounding case is presented in this feasibility study to highlight the maximum adaptation of the device in the proposed configuration.

2. Observer error formulation

In 1971, Beard introduced a Linear Time Varying (LTV) representation capable of describing time varying faults in a state space formulation (Beard 1971). Douglas later proposed that detection filters could be constructed in an observer framework to detect these faults (Douglas 1993). Recently, Chen and Nagarajaiah have developed and validated closed loop detection filters which are successful in detecting damage in LTV systems (Chen and Nagarajaiah 2008, Chen and Nagarajaiah 2008). An open loop observer formulation using a time segmented least squares approach for damage detection was developed and validated on experimental data by Nagarajaiah and Li (2004). Later, the open loop observer framework was augmented by a radial basis function decoupling by Contreras *et al.* and demonstrated robust detection of stiffness change for multi-degree of freedom systems and buildings (Contreras *et al.* 2011, Contreras *et al.* 2009). In this study, a basic open loop observer was used to adequately detect primary system stiffness change in real time. Since sensory data was observed at the top floor degree of freedom, the observer formulation is sufficient to detect changes in first mode behavior. The sensory data was produced by a laser displacement sensor. It is acknowledged that the basic open loop observer detection scheme focuses only on global changes in system parameters; however, for the demonstration of the ALP-STMD capabilities, the global detection is sufficient.

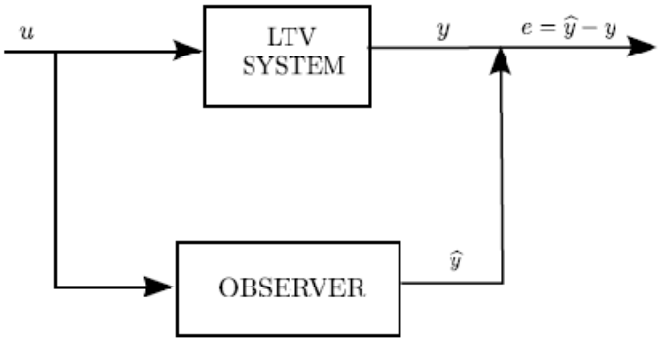

Fig. 1 Block diagram for open loop observer error

A block diagram of the open loop observer is illustrated in Fig. 1. The input excitation is fed simultaneously to the plant and to the observer. The output of both the healthy observer and the plant are compared in real time and form a residual error signal, $e = \hat{y} - y$. If the plant is modified in a time varying manner by a change in system stiffness and the model for the healthy observer is fairly accurate, then a nonzero residual error occurs with $e \neq 0$. If the plant remains unmodified in its nominal state, then the residual signal is zero, $e = 0$, for a system that is modeled perfectly, and close to zero for a system with bounded modeling errors.

The error function carefully monitors changes in the system. For the experiments performed in this study, if the error function increases to six times the nominal error bounds for a three second window of data, the frequency tracking controller proposed by Nagarajaiah and Pasala (2010) and Pasala and Nagarajaiah (2012) is engaged. The effective length of the ALP-STMD is changed in a manner such that it matches the frequency of the dominant response of the modified system. The tuned ALP-STMD is capable of absorbing the energy due to adaptation to suite the modified structure in real time based on the sensory feedback and the error estimation by the observer.

3. Experimental setup

A bench scale structural shear frame was selected for the experimental validations. The shear frame is the laboratory specimen developed in the companion paper (Pasala and Nagarajaiah 2012). It is constructed of 1/8 X 2 in. aluminum columns and 1/2 X 2 in. steel floor beams assumed to be rigidly connected by threaded screw joint connections in a 3:4 (floor:column) ratio. The system is excited at its base by a shaking table driven by a linear actuator controlled by dSPACE digital hardware and MATLAB/SIMULINK software. A laser displacement sensor is placed at the floor levels to capture the system response. The laser sensor provides relatively noise free, high fidelity data that affords the application of the proposed feedforward observer based real time system identification algorithm. The ALP-STMD is connected at the top floor. For further detail about the model, the reader is referred to the companion paper (Pasala and Nagarajaiah 2012).

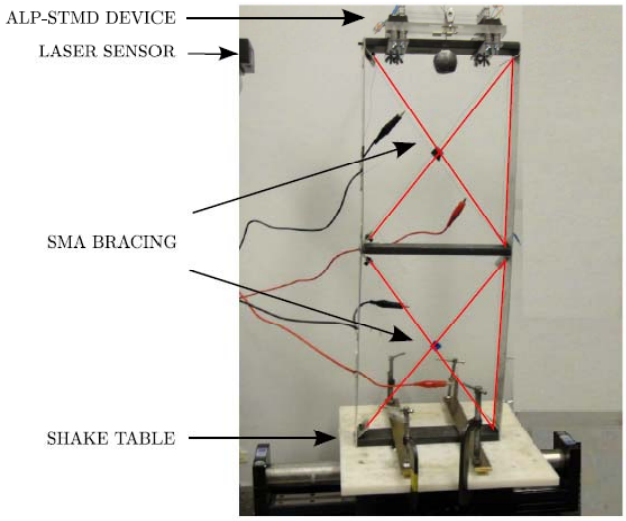

Fig. 2 Experimental setup with shape memory alloy bracing and ALP-STMD

The system is braced with Shape Memory Alloy wire (SMA) in a crossed-braced, continuous configuration which allows the time varying stiffness change in the shear frame to be generated from an elongation/relaxation of the brace length (see Fig. 2). The unique, superelastic properties of the SMAs enable the experiments to be performed repetitively without any permanent deformation to the SMA brace. Fig. 2 displays the complete experimental setup.

3.1 Device overview

The original development of an ALP was demonstrated by Nagarajaiah (2009) for a TMD which used a pulley system in combination with a rotary motor that could be controlled in real time. Pasala and Nagarajaiah and Nagarajaiah and Pasala later extended this idea to utilize the superelastic properties of the SMA wire and demonstrated its effectiveness in controlling first and second mode response for stationary, non-stationary, and impulse excitations (Nagarajaiah and Pasala 2010, 2012). The pulley system developed (Nagarajaiah and Pasala 2010) is composed of two rows of steel bearing, horizontal pulleys aligned in parallel that rest atop the second floor of the structure as shown in Figs. 3(a) and 3(b). The steel bearing, horizontal pulleys are secured using aluminum, conductive holders which allow the SMA wire to coil back and forth eventually securing to an 8 oz mass at one end of the wire. Also shown in Fig. 3(c), the mass is suspended over a vertical pulley with a certain amount of overhang pendulum length. The ability to vary the pendulum length to tune the period with the use of feedback is what makes the ALP-STMD a unique device.

The ALP is made possible by the crystalline structure material transition of the SMA wire. This material transition occurs at a critical phase transformation temperature. By passing an electrical current through the SMA wire, the resistive nature of the material induces Joule heating, which causes the temperature to rise. For this application, Nitinol (NiTi) SMA actuator wire with 0.010 mm diameter and a transition temperature of 90^{o}C was used in both the pendulum device

and floor braces. For the experiments, 0.80 A current was sufficient to raise the temperature of the SMA actuator beyond the transition temperature.

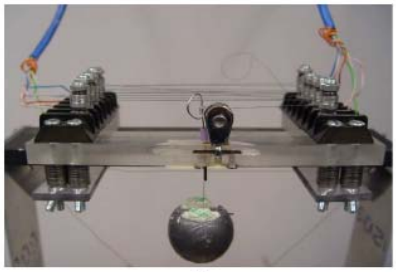

(a)

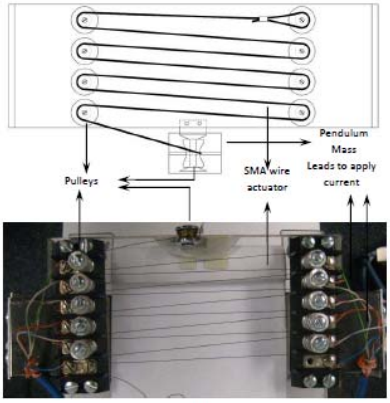

(b)

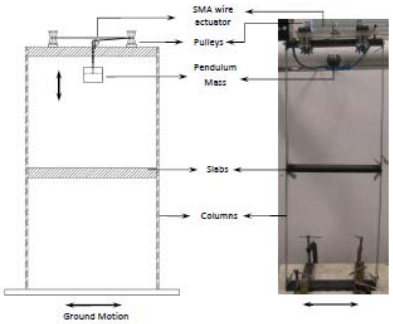

(c)

Fig. 3 (a) ALP-STMD, (b) SMA Wire for Pendulum Length Adjustments and (c) Schematic scaled two story model with ALP-STMD without SMA Bracing

When the current is zero, Joule heating does not occur and the SMA is in a superelastic state in which it is elongated by the weight of the mass. Consequently, the ALP has its greatest pendulum

length in these conditions, and energy will be transferred to the pendulum mass for a base excited system. When the current is increased, Joule heating causes the temperature to rise in the SMA wire. Once the critical transformation temperature is exceeded, the crystalline structure changes and the SMA wire returns to its intrinsic, contracted shape reducing the pendulum length of the ALP-STMD. If the pendulum length becomes zero, the ALP-STMD is not capable of absorbing energy of a base excited system and may be considered as an added mass to the second floor. If it is desired for practical purposes that when the current increases in the SMA wire so does the engaged length of the ALP-STMD pendulum, a mechanism has been proposed in the companion paper to obtain this behavior. The mechanism is not applied in this proof of concept study which is focused on adaptive tuning due to stiffness modification, but could be a concept in future applications.

A top view of the SMA pulley actuation device is shown in Figs. 3(a) and 3(b). This novel pulley configuration allows the variation of the effective length of the pendulum by passing current and applying heat through discrete portions of the overall wire length. By changing the terminals through which the current is sent, different lengths of the pendulum can be achieved. In general, exposing a greater portion of the SMA wire to heat will result in a greater portion of the pendulum length being contracted. Recalling Fig. 2, SMA braces are used to vary the period of the primary system in real time, and the ALP-STMD is used to control the response of the primary system by tuning it to the dominant response period.

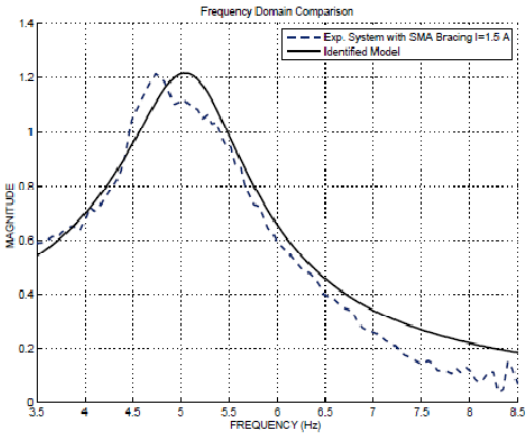

Fig. 4 Transfer function comparison (Experimental and identified)

3.2 Generating an observer model

Regarding system identification of the scaled two story model without the ALP-STMD engaged, the nominal state of the primary structural system was defined to be the stiffened state where 1.5 A of current was infused into each floor's SMA bracing (recall Fig. 2). This level of current in the SMA wire causes the temperature of the wires to remain high and consequently the braces taught with tension. Using a sine sweep base excitation, the modes of the stiffened system are excited. Due to the objectives of the experimental study, special consideration is afforded to capturing first

mode behavior. A transfer function, shown in Fig. 4, was produced describing the relationship between the response at the second floor and the input excitation.

Next, assuming the mass of the floors of the nominal system is known and assuming a standard shear frame, the stiffness and damping matrices are realized. The stiffness is represented by matrix, **K** with units (*N/m*), mass by a diagonal mass matrix, **M** in (*Kg*), and a banded Rayleigh damping matrix, $\mathbf{C}^{\text{damp}}$ with units (*N-sec/m*). The identified matrices for the healthy model are

$$\mathbf{K}=\begin{bmatrix} 7056 & -3456 \\ -3456 & 3456 \end{bmatrix} \qquad \mathbf{M}=\begin{bmatrix} 1.22 & 0 \\ 0 & 1.43 \end{bmatrix} \qquad \mathbf{C}^{damp}=\begin{bmatrix} 39.85 & 4.62 \\ 4.62 & -4.62 \end{bmatrix} \tag{1}$$

assuming the forms

$$\mathbf{K}=\begin{bmatrix} k_1+k_2 & -k_2 \\ -k_2 & k_2 \end{bmatrix} \qquad \mathbf{M}=\begin{bmatrix} m_1 & 0 \\ 0 & m_2 \end{bmatrix} \qquad \mathbf{C}^{damp}=\begin{bmatrix} c_1+c_2 & -c_2 \\ -c_2 & c_2 \end{bmatrix} \tag{2}$$

Once **M**, $\mathbf{C}^{damp}$, and **K** are realized, the open loop observer can be constructed from the controllable canonical state space representation with output displacement observed at the second floor as shown in Eq. (3).

$$\begin{aligned} \dot{\hat{\mathbf{x}}}_{4\times1}(t) &= \mathbf{A}_{4\times4}\hat{\mathbf{x}}_{4\times1}(t)+\mathbf{B}_{4\times1}u_{1\times1}(t) \\ \hat{y}_{1\times1}(t) &= \mathbf{C}_{1\times4}\hat{\mathbf{x}}_{4\times1}(t) \end{aligned} \tag{3}$$

The observer estimate of the state variable, $\hat{\mathbf{x}}_{4\times1}$, consists of a relative displacement vector for all degrees of freedom, $\hat{\mathbf{x}}_{2\times1}$, stacked on top of a relative velocity vector for all degrees of freedom, $\dot{\hat{\mathbf{x}}}_{2\times1}$. The input acceleration is $u_{1\times1}(t)$ and **A**, **B**, **C**, and are state space matrices defined as follows

$$\mathbf{A}_{4\times4}=\begin{bmatrix} \mathbf{0}_{2\times2} & \mathbf{I}_{2\times2} \\ -\mathbf{M}_{2\times2}^{-1}\mathbf{K}_{2\times2} & -\mathbf{M}_{2\times2}^{-1}\mathbf{C}_{2\times2}^{damp} \end{bmatrix} \tag{4}$$

$$\mathbf{B}_{4\times1}=\begin{bmatrix} \mathbf{0}_{2\times1} \\ \mathbf{\Gamma}_{2\times1} \end{bmatrix} \tag{5}$$

and

$$\mathbf{C}_{1\times4}=\begin{bmatrix} 0 & 1 & 0 & 0 \end{bmatrix} \tag{6}$$

where **Γ** is a vector of unity influence coefficients.

The analytical transfer function generated from the identified matrices compares well with the experimental transfer function as shown in Fig. 4. Since the nominal observer will be used in the time domain, a time history comparison is shown in Fig. 5. It is worth noting that although the model matches the phase behavior of the experimental output very well, there is some minor discrepancy in the approximation of magnitude. System noise and/or irregularities are most likely the cause of this phenomenon; however, as long as the magnitude of the approximation error is small relative to the overall response, it is deemed acceptable.

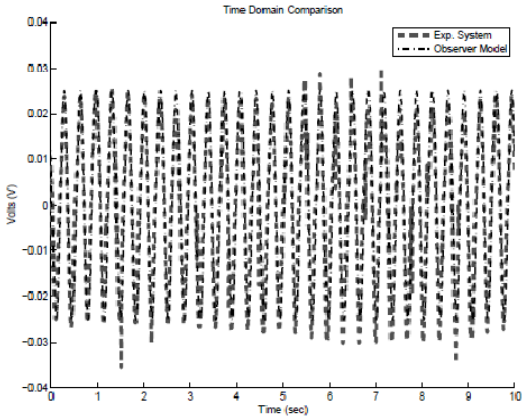

Fig. 5 Time domain comparison for 2nd floor response (Experimental system and identified observer model)

3.3 Using SMA to produce stiffness change

When the current in the SMA bracing is set to 0 A, the SMA braces are relaxed and they are no longer taught with tension (Fig. 2). This is considered the modified state because each floor has a changed stiffness. When stiffness is changed in the floors simultaneously, the properties of the structure will change. The change in system behavior is illustrated by the measured transfer functions from input to 2nd story displacement for both the nominal and modified state shown in Fig. 6.

The transfer functions produced in Fig. 6 were produced from chirp sine base excitation tests. The complete two story system with the ALP-STMD not engaged (in fixed configuration with zero length) was excited with a non-stationary sine sweep input. The second floor displacement was captured by the laser displacement sensor and the aforementioned transfer functions were obtained for the nominal and modified systems. The time history displacements for the second floor are shown in Fig. 7 for the chirp sine input. It is evident that the system experiences a resonant response at different frequencies for the nominal and modified systems.

The stiffness modified transfer function has a peak first mode response at 2.76 Hz and has a sharper peak in comparison to the nominal stiffness transfer function. The nominal system has a very broad, flattened first mode peak at 4.74 Hz. It is clear from the transfer function comparison data, that it is desirable to ensure that the structure remains in its nominal state for a first mode excitation. If the system is modified, it is the primary objective of the ALP-STMD to ensure the system response is reduced.

To illustrate the effect of the ALP-STMD on the stiffness modified system Fig. 8 shows the transfer function from input to 2nd story displacement of both the modified system with the ALP-STMD locked and the modified system with the ALP-STMD engaged. The figure was produced from data captured by chirp sine input excitation tests which are shown in Fig. 9. In Fig. 8, it is apparent that the ALP-STMD successfully distributes the total peak energy of the damaged system into two separate peaks over the frequency range of excitation. These two peaks are significantly smaller in magnitude than the peak frequency response of the stiffness modified system without ALP-STMD compensation (i.e. ALP-STMD in locked state).

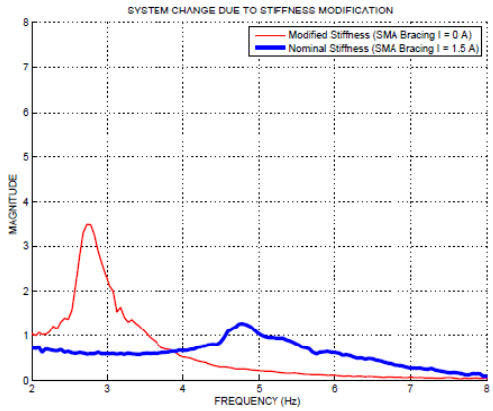

Fig. 6 Effect of stiffness modification on measured system transfer function

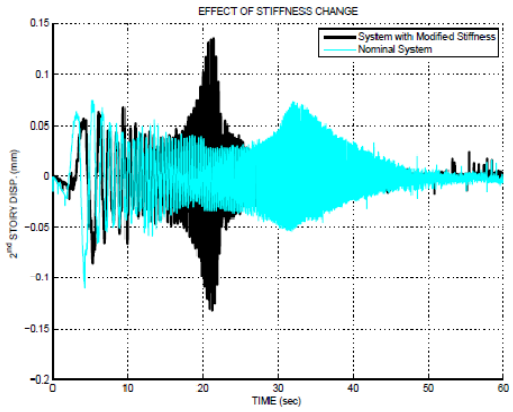

Fig. 7 Effect of stiffness modification: measured time domain response

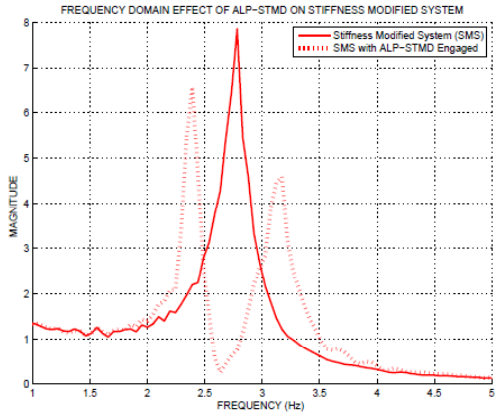

Fig. 8 Effect of ALP-STMD on stiffness modified system: FRF comparison

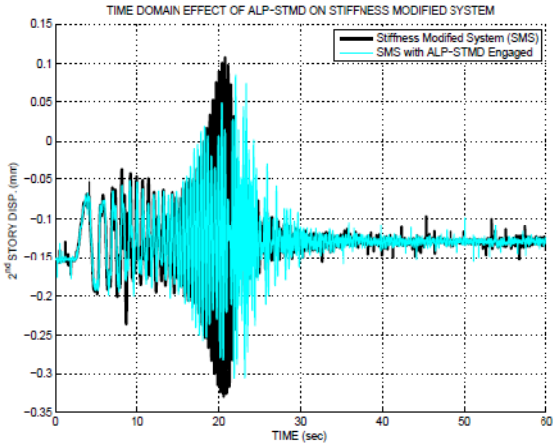

Fig. 9 Effect of ALP-STMD on stiffness modified system: time domain comparison

4. Experimental results

The experimental procedure that validates the proposed control algorithm and demonstrates the benefits of implementing the ALP-STMD is described next. The structural system was excited with a stationary sinusoidal base excitation oscillating at 2.75 Hz. At time t = 15 sec, the SMA brace current was shut off/set to 0 A to induce a stiffness modification in the system. In real time, the system was being monitored by the error function introduced in Section 2, which utilized the identified analytical model presented in Section 3.2. When the error function threshold was exceeded, the ALP-STMD was engaged in real time and tuned to the dominant frequency present in the response using the STFT control algorithm presented by Pasala and Nagarajaiah (Pasala and Nagarajaiah 2012) and Nagarajaiah and Pasala (2010). The error function results are displayed for 60 seconds of experimental data in Fig. 10.

From time 0-15 seconds the error function oscillates between a nominal max/min value close to zero that is associated with the nominal system. After time 15 seconds, the system passes through a short transition zone in which heat is dissipating from the SMA bracing and the tension decreased. After the SMA bracing has cooled to its modified stiffness state, the entire structural system experiences a larger displacement which is evidenced by the error function exceeding the controller threshold of 0.15 V after 32 seconds. After the threshold has been exceeded for the duration of the proposed window length of 3 seconds, the ALP-STMD frequency tracking algorithm is activated.

In Figs. 11 and 12 respectively, the 2nd and 1st floor displacement time history responses are displayed in the presence of the stiffness modification and ALP-STMD activation. The frequency tracking is triggered at 35 seconds. After 3 seconds of tracking the dominant vibration frequency, the current in the ALP-STMD device is set to 0 A at nearly 39 seconds to match the optimal length required to match the dominant frequency of vibration. The response at both floors is reduced immediately as evident in Figs. 11 and 12.

The 2nd and 1st floor displacements were reduced by as much as 57 \% and 47 \% respectively. It is important to note that these reductions were still achieved despite a nominal tuning of the

ALP-STMD. A finer tuned system would reduce the off frequency `beating' that is evident in Figs. 11 and 12. Finally in Fig. 13, open and closed loop responses for each floor are shown. It is apparent from the Fig. 13 that despite stiffness modification due to the SMA bracing in each floor, the structural frame experienced significantly reduced response due to deployment of the ALP-STMD when compared to a system without ALP-STMD and such adaptive benefits.

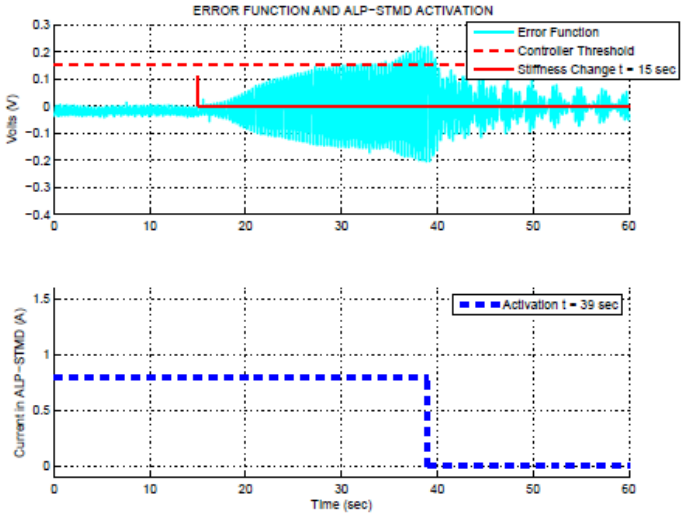

Fig. 10 Error and ensuing ALP-STMD activation in the presence of stiffness change

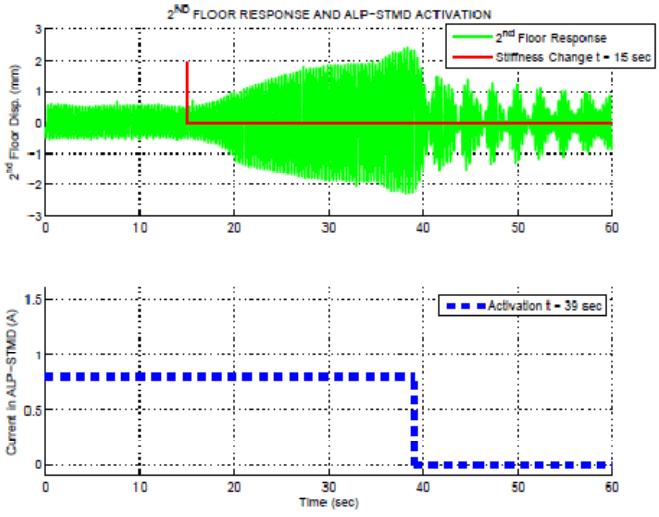

Fig. 11 Effect of ALP-STMD on 2nd floor displacement

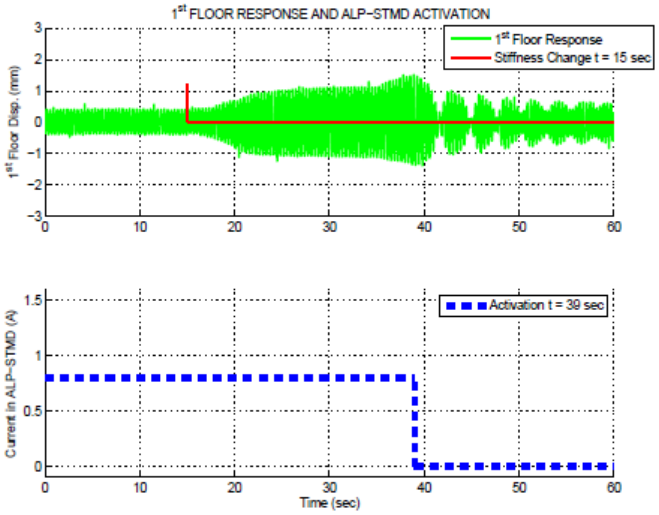

Fig. 12 Effect of ALP-STMD on 1st floor displacement

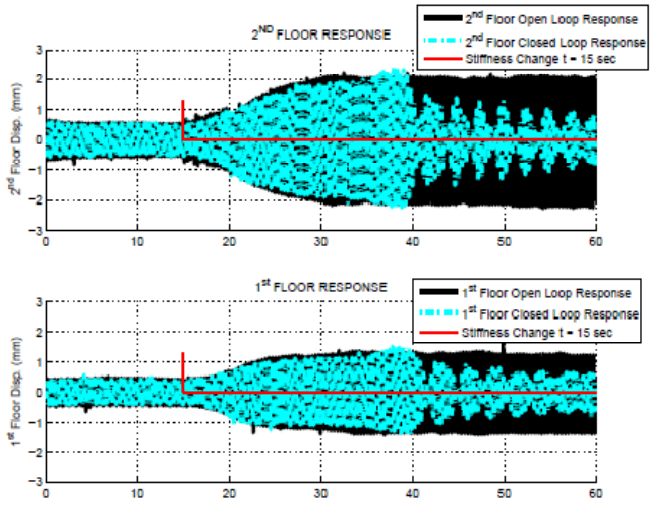

Fig. 13 Open loop and closed loop comparison for each floor

5. Conclusions

A proof of concept experimental study involving real time system identification and adaptive tuning of the newly developed ALP-STMD was performed. It was validated with an open loop observer formulation that (1) is capable of identifying the structural stiffness changes of the bench scale specimen in real time and (2) could be incorporated as an activation trigger for semi-active

structural control of the ALP-STMD. A stiffness change was induced in real time to the primary system by regulating current flow to SMA brace wires in the first and second floor of the structure. This stiffness modification scenario utilized the superelastic nature of SMA materials so that the test could be performed repetitively without any yielding of the material. In the presence of stiffness change and base excitation, the ALP-STMD showed favorable performance with respect to magnitude of the 2nd and 1st floor response reduction.

Acknowledgements

The authors would like to acknowledge support from the National Science Foundation through cooperative agreement no. CMMI-0830391. Additionally, the first author gratefully acknowledges the National Science Foundation for its support through the Alliance for Graduate Education and the Professoriate fellowship program, cooperative agreement no. HRD-0450363.

References

Abe, M. and Igusa, T. (1996), "Semi-active dynamic vibration absorbers for controlling transient response", *J. Sound Vib.*, **1998**(5), 547-569.

Beard, R.V. (1971), *Failure accommodation in linear system through self reorganization*, PhD Thesis, Massachusetts Institute of Technology.

Caughey, T.K. and Karyeaclis, M.P. (1989), "Stability of semi-active impact damper, part I-global behavior; part II-periodic solutions", *J. Appl. Mech - T ASME*, **56**(4), 926-940.

Chen, B. and Nagarajaiah S. (2008a), "Structural damage detection using decentralized controller design method", *Smart Struct. Syst.*, **4**(6), 779-794

Chen, B. and Nagarajaiah S. (2008b), "H_2/H_∞ structural damage detection filter design using iterative LMI approach", *Smart Mater. Struct.*, **17**(3), 03501.

Contreras, M., Nagarajaiah, S. and Narasimhan S. (2009), "Real time damage detection in buildings using filter based radial basis function network mapping", *Proceedings of the ASCE Struct. Eng. Instit.*, Austin, TX, May.

Contreras, M., Nagarajaiah, S. and Narasimhan, S. (2011), "Real time detection of stiffness change using a radial basis function augmented observer formulation", *Smart Mater. Struct.*, **20**(3), 035013.

Douglas, R.K. (1993), *Robust fault detection filter design*, PhD Dissertation, The University of Texas at Austin.

Hazra, B., Sadhu, A., Lourenco, R. and Narasimhan, S. (2010), "Re-tuning tuned mass dampers using ambient vibration measurements", *Smart Mater. Struct.*, **19**, 115002.

Hrovat, D., Barak, P. and Rabins, M. (1983), "Semi-active versus passive or active tuned mass dampers for structural control", *J. Eng. Mech. - ASCE*, **109**(3), 691-705.

Ikeda, Y., Sasaki, K., Sakamoto, M. and Kobori, T. (2001), "Active mass driver system as the first application of active structural control", *Earthq. Eng. Struct. D.*, **30**(11), 1575-1595.

Koike, Y. and Tanida, K. (1998), "Application of V-shaped hybrid mass damper to high rise buildings and verification of damper performance", *Proceedings of the Structural Engineers World Congress*, San Francisco, CA, T198-4.

Lou, J.Y.K., Lutes, L.D. and Li, J.J. (1994), "Active tuned liquid damper for structural control", *Proceedings of the 1st World Conf. on Structural Control*, Los Angeles, CA, TP1: 70-9.

Mekki, O., Ben, Bourquin, F., Maceri, F. and Van Phu, C. Nguyen. (2011), "An adaptive pendulum for evolving structures", *Struct. Control Health Monit.*, **19**(1), 43-54.

Meli R., Faccioli E., Murià-Vila D., Quaas R. and Paolucci R., (1998) "A study of site effects and seismic response of an instrumented building in Mexico City", *J. Earthq. Eng.*, **2**(1), 89-111.

Muria-Vila, D., Fuentes Olivares, L., and Gonzalez Alcorta, R. (2000), "Uncertainties in the estimation of natural frequencies of buildings in Mexico City", *Proceedings of the 12th World Conf. on Earthquake Engineering*, Auckland, N. Z.

Nagarajaiah, S. and Varadarajan, N. (2000), "Novel semiactive variable stiffness tuned mass damper with real time tuning capability", *Proceedings of the 13th Engineering Mechanics Conf.*, CD-ROM, Reston, VA.

Nagarajaiah, S. and Li, Z. (2004), "Time segmented least squares identification of base isolated buildings", *Soil Dyn. Earthq. Eng.*, **24**(8), 577-586.

Nagarajaiah, S. (2009), "Adaptive passive, semiactive, smart tuned mass dampers: identification and control using empirical mode decomposition, Hilbert Transform, and Short-Term Fourier Transform", *Struct. Control Health Monit.*, **16**(7-8), 800-841.

Nagarajaiah, S. and Pasala, D.T.R. (2010), "Adaptive length pendulum dampers", *Proceedings of the ASCE Structures Congress*, CD-ROM.

Nagarajaiah, S., Pasala, D.T.R. and Huang, C. (2010), "Smart TMD: adaptive length pendulum damper", *Proceedings of the 5th World Conference on Structural Control and Monitoring*.

Occhiuzzi, A., Spizzuoco, M. and Ricciardelli, F. (2008), "Loading models and response control of footbridges excited by running pedestrians", *Struct. Control Health Monit.*, **15**(3), 349-368.

Pasala, D.T.R. and Nagarajaiah, S. (2012), "Adaptive-length pendulum smart tuned mass damper using shape-memory -alloy for real-time tuning", *Smart Struct. Syst.*, (accepted).

Peterson, N.P. (1980), *Design of large scale tuned mass dampers*, Structural Control, North Holland Publishing Company, Amsterdam, Netherlands.

Roffel, A.J., Lourenco, R. and Narasimhan, S. (2010),"Experimental studies on an adaptive tuned mass damper with real-time tuning capability", *Proceedings of the ASCE Conference*, **370**(41131), 27.

Roffel, A., Lourenco, R., Narasimhan, S. and Yarusevych, S. (2011), "Adaptive compensation for detuning in pendulum tuned mass dampers", *J. Struct.Eng. - ASCE*, **137**(2), 242-251.

Varadarajan, N. and Nagarajaiah, S. (2004), "Wind response control of building with variable stiffness tuned mass damper using empirical mode Decomposition/Hilbert Transform", *J. Eng. Mech.- ASCE*, **103**(4), 451-458.

Weber, F., Boston, C. and Maslanka, M. (2011), "An adaptive tuned mass damper based on the emulation of positive and negative stiffness with an MR damper", *Smart Mater. Struct.*, **20**(1), 015012.

Yalla, S., Kareem, A. and Kantor, C. (2001), "Semiactive tuned liquid dampers for vibration control of structures", *Eng. Struct.*, **23**(11), 1469-1479.